

PACS numbers: 42.62.Cf; 81.05.Bx
DOI: 10.1070/QE2000v030n09ABEH001814

Dynamics of the egress of gas microbubbles from a melt under laser irradiation of a metal surface

V V Likhanskii, A I Loboiko

Abstract. The results of a theoretical investigation of the efficiency of degassing of the near-surface region of a material exposed to laser radiation are presented. The case of a low volume concentration of the monodispersed gas phase representing microbubbles of size no greater than 10 μm is considered. The principal parameters are revealed which determine the regimes of the egress of gas bubbles from a laser-produced melt, and analytical formulas are obtained for estimating the process rate. The analytical results are compared with the results of two-dimensional numerical simulations which include the laser heating of a solid sample, its melting, the development of thermocapillary melt convection, and the escape of gas bubbles from the melt. The analytical and numerical results are found to be in good agreement.

1. Introduction

One of defects occurring frequently in welding materials is microscopic gas pores, which significantly impair the quality of a welded joint and, hence, the durability of weld-fabricated structures. There exist different empirical ways to eliminate the defects of this kind: the use of a gas-forming fusing agent at the ends of the edges of a construction to be welded [1], laser remelting of welded joints [2], and other techniques.

However, a radical solution of the problem is unfeasible without gaining a qualitative understanding of the physical processes that occur in the molten pool and quantitative criteria to allow making a trustworthy prediction of the result. This work is devoted to a theoretical study of the dynamics of the egress of gas microbubbles from a melt produced by laser irradiation of a metal surface.

2. Theoretical analysis

A specific feature of laser action is attainment of high temperature gradients in the melt. The bubbles in a molten pool move under the action of the buoyancy force [3], due to their entrainment by the hydrodynamic flow [4], and owing to thermocapillary drift [5, 6]. The latter mechanism, which is caused by the temperature dependence of surface tension and the nonuniformity of heating of the bubble surface in the absence of surface-active impurities, may play a decisive role in the process of degassing of the laser melt.

The velocity of a steady-state thermocapillary bubble drift for small Reynolds numbers was found in Refs [5, 6]. When a material is melted by laser radiation, the regime of bubble motion for large Reynolds numbers is usually realised because high temperature gradients cause a significant nonuniformity of heating of the bubble surface.

This regime was investigated analytically in Ref. [5] without inclusion of the bubble-melt heat exchange and in Ref. [7], taking this heat exchange into account. The velocity of the carrier phase was assumed to be uniform and the temperature gradient to be constant. In reality, the inclusion of thermocapillary convection leads to complex nonuniform distributions of the temperature and the melt velocity.

In particular, the temperature gradient under laser irradiation is directed from the periphery to the centre of the molten pool. At the same time, the thermocapillary flow of the melted material in the near-surface layer occurs, as a rule, from the centre to the periphery, while in the benthal region, it occurs in the opposite direction. As a result, the forces act on a gas bubble in one direction near the bottom and in different directions in the near-surface region. Therefore, the type of motion of a gas bubble in the molten pool is substantially determined by the parameters of laser radiation.

The dynamics of laser degassing may be conventionally divided into three stages: formation of bubbles in the melt, their floating up and passage through the melt surface. The first and partly second stages were studied in Refs [1, 8], while the last stage was never analysed. A gas bubble passes through the melt surface not instantaneously and, if the degassing is to be effective, the characteristic residence time t^* of a gas bubble in the near-surface region should exceed the characteristic passage time. Otherwise the convective flows of the melted material would carry the bubble to the pool periphery where it can either be carried deep into the melt or fixed as a pore during solidification of the melt.

To estimate t^*, we consider the motion of a single bubble and neglect its effect on the motion of the melt, which is valid for small bubble dimensions and a low concentration of the gas phase. Then, the motion of the gas bubble is described by the equation [9]:

$$\frac{4}{3}\pi r_b^3 \rho_b \frac{dU_b}{dt} = F_{fr} + F_{tc} + F_{ar} + F_{am}, \quad (1)$$

where r_b, ρ_b, and U_b are the bubble radius, its density and

V V Likhanskii, A I Loboiko Troitsk Institute for Innovation and Thermonuclear Research (State Scientific Centre of the Russian Federation), 142092 Troitsk, Moscow oblast, Russia

Received 30 March 2000
Kvantovaya Elektronika **30** (9) 827 – 832 (2000)
Translated by E N Ragozin; edited by M N Sapozhnikov

velocity, respectively; F_{fr} is the frictional force acting on the bubble in the melt; F_{tc} is the thermocapillary force; F_{ar} is the buoyancy force; and F_{am} is the associated mass force. The frictional force F_{fr} acting on the bubble in the melt has the form [10]

$$F_{fr} = \frac{4}{3}\pi r_b^3 \rho_b G(U_f - U_b),$$
$$G = \frac{3}{8} C_{fr} \frac{\rho_f}{\rho_b} \frac{1}{r_b} |U_f - U_b|, \tag{2}$$

where C_{fr} is the friction coefficient; U_f and ρ_f the flow velocity of the carrier phase (the melt) at the location of the bubble and the carrier phase density, respectively. Here, we analyse first of all the motion of microbubbles with $r_b < 0.1$ mm. In this case, the bubble motion under laser melting of a metal is characterised by a small Weber number $We = r_b \rho_f (U_f - U_b)^2/\sigma \ll 1$ (where σ is the surface tension coefficient of the melt) and the bubble is spherical. For Reynolds numbers $1 < Re_b < 500$, the friction coefficient is described by the formula $C_{fr} = 48(1 - 2.2/Re_b^{0.5})/Re_b$ (in the subsequent estimates, we used the approximation $C_{fr} \approx 48/Re_b$), and for $Re_b \ll 1$, by the relationship $C_{fr} = 16/Re_b$, where $Re_b = 2r_b|U_f - U_b|/v$ [10]; v is the coefficient of kinematic viscosity.

The thermocapillary force F_{tc} has the form [5]

$$F_{tc} = F_0 \pi r_b^2 \gamma \frac{\partial T}{\partial r}. \tag{3}$$

Here, $\partial T/\partial r$ is the temperature gradient at the location of the bubble; $\gamma = |\partial\sigma/\partial T|$; $F_0 = 4$ for $Re_b > 1$, and $F_0 = 3$ for $Re_b \ll 1$.

The buoyancy force F_{ar} and the associated mass force F_{am} are determined by the expressions [10]

$$F_{ar} = \frac{4}{3}\pi r_b^3 \rho_f \left(\frac{dU_f}{dt} - g\right), \tag{4}$$

$$F_{am} = \frac{2}{3}\pi r_b^3 \rho_f \left(\frac{dU_f}{dt} - \frac{dU_b}{dt}\right), \tag{5}$$

where g is the gravitational acceleration.

To analyse the bubble motion near the free melt surface, the velocity of melt motion and the temperature gradient in the near-surface region should be estimated. For this purpose, we will use the exact solution of the problem of thermocapillary melt convection for a Gaussian intensity distribution in the focal spot [11]:

$$U_f(r) = \left(\frac{2C\gamma}{\rho_f^2 v C_f}\right)^{1/2} \left(\frac{W}{r_0^2}\right)^{1/2} r,$$
$$\frac{\partial T}{\partial t}(r) = -\left(\frac{8C^3}{\rho_f^2 \gamma v C_f^3}\right)^{1/4} \left(\frac{W}{r_0^2}\right)^{3/4}, \tag{6}$$

where W is the intensity of laser radiation absorbed by the surface; r_0 is the characteristic dimension of the Gaussian distribution; C_f is the heat capacity of the melt; and $C = 0.35$ is the constant of the analytical solution. Substituting expressions (2)–(6) in Eqn (1) and taking into account that $\rho_b \ll \rho_f$, we obtain the equation of bubble motion in the near-surface melt layer:

$$\frac{d^2 r}{dt^2} + 18 t_m^{-1} \frac{dr}{dt} + \left(6 t_m^{-1/2} t_u^{-3/2} - 18 t_m^{-1} t_u^{-1} - 3 t_u^{-2}\right) r = 0, \tag{7}$$

where

$$t_u = \left(\frac{2C\gamma}{\rho_f^2 v C_f}\right)^{-1/2} \left(\frac{W}{r_0^2}\right)^{-1/2} \tag{8}$$

is the characteristic convection time of the melt and $t_m = r_b^2/v$ is the characteristic time taken to entrain a bubble in the motion of the carrier phase.

From the solution of (7), which has the form $r(t) \sim C_1 \exp(t/t^*) + C_2 \exp(t/t^{**})$, and the initial conditions, it follows that C_1, C_2, $t^* > 0$ and $t^{**} < 0$ [where $1/t^*$ and $1/t^{**}$ are the first and second roots of the characteristic equation of the differential equation (7)] for arbitrary parameters of the laser radiation and the bubble size. The estimate of the characteristic residence time of a gas bubble at the melt surface t^* gives

$$t^* = \frac{t_m}{9\left[(1+B)^{1/2} - 1\right]},$$
$$B = \frac{1}{81}\left[3\left(\frac{t_m}{t_u}\right)^2 - 6\left(\frac{t_m}{t_u}\right)^{3/2} + 18\left(\frac{t_m}{t_u}\right)\right]. \tag{9}$$

Two limiting cases may be considered in the analysis of (9): quick ($B \ll 1$ or $t_m \ll t_u$) and slow ($B \gg 1$ or $t_m \gg t_u$) entrainment of a bubble in the near-surface melt convection. In the former case, the time t^* is independent of the bubble size and is equal to the characteristic convection time of the melt: $t^* \approx t_u$. In the latter case, the time t^* also does not depend on the bubble size but is slightly shorter than the characteristic convection time: $t^* \approx 3^{-1/2} t_u \approx 0.577 t_u$.

Hence it follows that, for a developed thermocapillary melt convection, no parameters of laser radiation exist at which a gas bubble moves towards the centre of the molten pool in the near-surface region when the temperature gradient points toward the centre of the focal spot. For a thermocapillary convection, the escape of a gas bubble from the melt may be hindered if the bubble residence time t^* at the melt surface is shorter than the characteristic time t_{out} of the bubble passage through the melt surface.

Consider the efficiency of degassing of a molten pool with a low volume concentration α_0 of the gas phase in a sample ($\alpha_0 \ll 1$) for laser radiation parameters typical for melting. Let the bubbles of the gas phase be of the same size. Then, the number N_b of bubbles in the melt at the melting stage varies according to the equation

$$\frac{dN_b}{dt} = \alpha_0 \frac{dV}{dt} - \frac{N_b}{\tau},$$

where $V(t)$ is the volume of the molten pool; τ is the characteristic residence time of a gas bubble in the melt. The first term on the right describes the arrival of gas bubbles to the pool of liquid due to melting of the solid phase, and the second term describes the escape of bubbles from the molten pool through the free surface. In view of the relationship $N_b = \alpha(t)V(t)$, the variation in the volume gas concentration in the melt may be represented in the form

$$\frac{d\alpha}{dt} = (\alpha_0 - \alpha)\frac{1}{V}\frac{dV}{dt} - \frac{\alpha}{\tau}. \quad (10)$$

The total residence time τ of a gas bubble in the melt is composed of the drift time t_{int} of a bubble from the bottom of the pool to the surface and the time t_{out} of passage of a bubble through the free surface: $\tau = t_{int} + t_{out}$. Let the characteristic time t_{out} depend on the bubble size and the physical characteristics of the melt surface which are invariable throughout the lifetime of the melt. The characteristic time is $t_{int} \sim h(t)/u_{int}$, where $h(t)$ is the time-dependent depth of the pool of the melt and u_{int} is the vertical bubble velocity.

Note that for $\alpha_0 \ll 1$, the dependence of the thermal properties of the sample on the concentration of the gas phase may be neglected. Then, in the initial stage of melting, the volume of the melt increases proportionally to time, the proportionality coefficient depending on the parameters of laser radiation and the thermal properties of the sample, i. e.,

$$\frac{1}{V(t)}\frac{dV}{dt} \simeq 1/t$$

for different regimes of laser irradiation. Using this relationship, consider two limiting regimes of the egress of bubbles from the melt.

For $t_{int} \ll t_{out}$, Eqn (10) can be rewritten in the form

$$\frac{d\alpha}{dt} = \frac{\alpha_0 - \alpha}{t} - \frac{\alpha}{t_{out}}.$$

This expression for $t_{out} \equiv \text{const}$ is easily integrated and, for the initial conditions $\alpha(t = 0) = \alpha_0$, we obtain

$$\frac{\alpha(t)}{\alpha_0} = \left[1 - \exp\left(-\frac{t}{t_{out}}\right)\right]\frac{t_{out}}{t}. \quad (11)$$

Note that the degree of degassing of the pool of the melt depends, under the assumptions made, only on the time of passage of a bubble through the melt surface and is independent of the parameters of laser radiation, even though the formation rate and the volume of the pool of melt depend on these parameters.

For $t_{int} \gg t_{out}$, we will use the correlation relationship for the melt depth in the initial stage of melting $h(t) \sim t^{1/2}$. Then, the characteristic time a bubble takes to float from the bottom of the pool to the surface is estimated as

$$t_{int} = \frac{h_{max}}{u_{int}}\left(\frac{t}{t_{max}}\right)^{1/2} = \beta t^{1/2}, \quad (12)$$

where h_{max} is the maximum depth of the pool of melt attained by the end of the radiation pulse of length t_{max}. Furthermore, early in the melting the vertical bubble velocity u_{int} is close to the drift thermocapillary velocity u_{dr}, because the vertical component of the thermocapillary force exceeds the buoyancy force by several orders of magnitude:

$$u_{int} \approx u_{dr} = D\frac{r_b}{\rho_f \nu}\gamma\frac{W}{\kappa}, \quad (13)$$

where κ is the thermal conductivity coefficient; $D = 1/3$ for $Re_b \gg 1$ and $D = 1/2$ for $Re_b \ll 1$ [5]. In view of the assumptions made above, Eqn (10) is written as

$$\frac{d\alpha}{dt} = \frac{\alpha_0 - \alpha}{t} - \frac{\alpha}{\beta t^{1/2}}. \quad (14)$$

With the initial condition $\alpha(t = 0) = \alpha_0$, the solution of Eqn (14) is given by the expression

$$\frac{\alpha(t)}{\alpha_0} = \frac{\beta^2}{2t}\left[\exp\left(-\frac{2t^{1/2}}{\beta}\right) + \frac{2t^{1/2}}{\beta} - 1\right]. \quad (15)$$

Compare now analytical expressions (11) and (15) with the results of two-dimensional numerical simulations which include laser radiation heating of a solid sample with a low concentration of the monodispersed gas phase, its melting, the appearance of thermocapillary convection, and the motion and the escape of gas bubbles from the melt.

3. Numerical results

To model the two-phase convection of the bubbles-melt heterogeneous mixture, we used a computation scheme based on a continuous representation of the carrier medium and discrete representation of the dispersed phase. The bubble motion was simulated by Eqns (1) – (5). The melt was assumed to be a viscous incompressible heat-conducting liquid whose dynamics was described by the continuity and Navier – Stokes equations in the Boussinesq approximation taking into account the forces which the gas bubbles exert on the heat carrier [10]:

$$\frac{\partial \eta}{\partial t} + \operatorname{div} \eta U_f = 0, \quad (16)$$

$$\frac{\partial U_f}{\partial t} + U_f \operatorname{grad} U_f = -\frac{1}{\rho_f}\operatorname{grad} p + \frac{1}{\eta}\operatorname{div}(\eta \nu \operatorname{grad} U_f) + \frac{F_v}{\eta \rho_f}, \quad (17)$$

$$\frac{\partial \eta C_f \rho_f T}{\partial t} + \operatorname{div}(\eta C_f \rho_f T U_f) = \operatorname{div}(\eta \kappa_{ef} \operatorname{grad} T) + F_T, \quad (18)$$

where $\eta = 1 - \alpha$ is the volume fraction of the melt; F_v and F_T are the terms that take into account the momentum and heat exchanges between a unit volume of the melt and the gas bubbles, respectively; κ_{ef} is the effective thermal conductivity coefficient of the melt-gas bubbles mixture; and p is the pressure in the liquid.

The equation for the temperature distribution in the solid phase has the form

$$C_s \rho_s \frac{\partial T}{\partial t} - \operatorname{div}(\kappa_{ef} \operatorname{grad} T) = 0, \quad (19)$$

where C_s and ρ_s are the heat capacity and the density of the solid phase, respectively. The solid-melt phase transition and the boundary conditions are taken into account in a conventional way like, e. g., in Ref. [12]. In the present calculations, we neglected the terms describing the interphase exchange because of a low volume concentration of the gas phase. In addition, we also neglected the dependence of thermal properties of the sample on the gas phase concentration.

The numerical model developed to correctly describe the degassing of the pool of melt upon thermocapillary convection under laser irradiation is based on the well known Lagrange – Euler technique of solution. The Navier – Stokes equations for a viscous incompressible liquid (16) – (18) and the equation for the temperature of the carrier phase (19) are solved by the Euler method on an immobile difference

grid. The Lagrange method is employed to solve the Boussinesq – Oseen equation (1) for the motion of a gas bubble in the melt. In this case, the physical parameters determined on the Eulerian difference grid, which are required to calculate the motion of a Lagrangian particle (a bubble), are interpolated at the location of this particle. This method of solution simulates with good accuracy the motion of the gas bubble in the pool of melt and was previously employed in the calculations of heat transfer through a liquid layer in bubbling [13].

Below, we present the results of calculations for the laser radiation with a Gaussian intensity distribution in the spot, a beam radius $r_0 = 0.1$ cm, and a pulse duration $t_{max} = 0.1$ s for an absorbed radiation power $P_0 = 500$ W. The thermal parameters of the sample were assumed to be temperature-independent: $\rho_f = 7.8$ g cm^{-3}, $C_f = 0.56$ J K^{-1} g^{-1}, $\kappa = 0.4$ W K^{-1} g^{-1}, $\nu = 5.5 \times 10^{-3}$ cm^2 s^{-1}, $\gamma = 0.35$ dyn K^{-1} $\times$cm^{-1}, a melting point of 1730 K, and a specific phase transition energy of 2184 J cm^{-3}. The initial distribution of gas-filled pores was assumed to be uniform over the entire volume of the sample while the pore size was varied in the calculations from 0.1 to 10 μm. We used in the numerical simula-tions a nonuniform rectangular difference grid, which had 100×100 cells and was thickened upon approaching to the free surface to more precisely approximate the boundary conditions, and 3500 discrete particles describing the motion of gas bubbles. The characteristic time t_{out} a gas bubble takes to pass through the melt surface was varied in the calculations from 10^{-2} to 10^{-4} s.

The calculations showed that for short t, the flow has a conventional single-vortex structure: in the near-surface layer, the melt moves from the centre to the periphery and in the benthal region in the opposite direction. In this case, the characteristic residence time of a gas bubble in the near-surface region of the melt correlates well with the theoretical estimate. The characteristic time t_u calculated by formula (8) is, for the given parameters of the problem, 6.6×10^{-4} s. As a result, in a time $t_{out} = 10^{-4}$ s, the gas bubbles, having reached the surface, had time to escape from the melt prior to being pulled by the flow to the periphery of the pool. In a time $t_{out} = 10^{-2}$ and 10^{-3} s, the reverse situation was realised: the drift to the periphery occurred faster than the escape from the melt. Consider in greater detail the degassing dynamics of the pool of melt for different bubble dimensions.

Bubbles 10 μm in radius. In the calculations, the phase of sample heating lasts, to the onset of melting, till the moment $t_{melt} \sim 0.0106$ s, which is in good agreement with formula (15). By the end of the laser pulse, the calculated depth of the pool of melt attains $h_{max} \sim 230$ μm. For $t_{melt} < t < t_{melt} + t_{out}$, the bubbles are accumulated on the free melt surface and next, for $t > t_{melt} + t_{out}$, the bubbles escape from the pool. An estimate of the floating velocity for the bubbles of this size gives $u_{int} \approx 100$ cm s^{-1} for the values of the physical parameters selected. In this case, the maximum time attained by the end of the laser pulse is $t_{int} = h_{max}/u_{int} = 2.3 \times 10^{-4}$ s and, hence, for $t_{out} = 10^{-2}$ and 10^{-3} s, the dynamics of the egress of gas bubbles from the melt should be described by expression (11). Fig. 1a gives a comparison of the numerical calculations with the analytical dependence (11), which demonstrates the validity of the above assumptions.

Bubbles 1 μm in radius. The floating velocity for the bubbles of this size is $u_{int} \approx 10$ cm s^{-1}. As a result, the maximum $t_{int} \approx 2.3 \times 10^{-3}$ s, and the gas bubble egress for $t_{out} = 10^{-2}$ s should be described by expression (11) as before. However, for $t_{out} = 10^{-3}$ s, the time $t_{int} = \beta t^{1/2}$ changes during melting from $t_{int} < t_{out}$ in the initial stage of the egress of bubbles to $t_{int} > t_{out}$ at the end of the laser pulse. In this case, the solutions (11) and (15) cannot be used formally. However, if we recall that the total time of the egress of bubbles from the melt is $\tau = t_{int} + t_{out}$ and substitute the averaged value $t_{int} \approx t_{out}$ in this relationship, we obtain the approximate dependence:

$$\frac{\alpha(t)}{\alpha_0} \approx \left[1 - \exp\left(-\frac{t}{2t_{out}}\right)\right] \frac{2t_{out}}{t}. \qquad (20)$$

A comparison of the numerical calculations with dependence (11) for $t_{out} = 10^{-2}$ s and with dependence (20) for $t_{out} = 10^{-3}$ s (Fig. 1b) confirms the assumption made above.

Bubbles 0.1 μm in radius. For bubbles of this size, $Re_b \ll 1$, and therefore the floating velocity is $u_{int} \approx 1.5$ cm s^{-1}, while formula (12) gives the coefficient $\beta \approx 5 \cdot 10^{-2}$ s$^{1/2}$. The maximum $t_{int} \approx 1.5 \times 10^{-2}$ is comparable to $t_{out} = 10^{-2}$ s; hence, by analogy with the previous case, approximate expression (20) is to be used to describe the dynamics of the escape of bubbles from the melt. For $t_{out} = 10^{-3}$ s, the characteristic time $t_{int} = \beta t^{1/2}$ exceeds t_{out} throughout the temporal range — from the moment at which the bubbles commence to escape from the melt to the end of the laser pulse. In other words, the dynamics of the egress of bubbles should be described by expression (15). These analytical dependences are given in Fig. 1c and demonstrate good agreement with the corresponding numerical calculations.

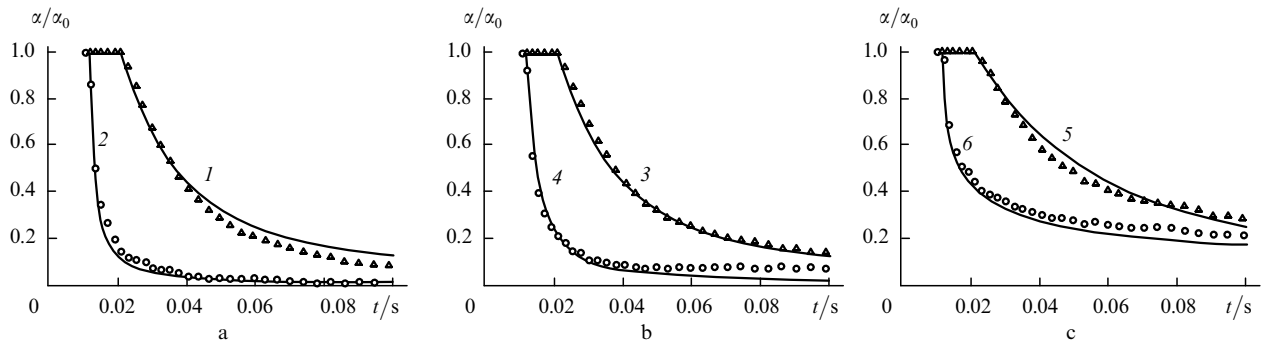

Figure 1. Numerical (circles and triangles) and analytical (curves) calculations of the time dependences of the volume concentration of the gas phase in the pool of melt for gas bubbles with a radius 10 (a), 1 (b), and 0.1 μm (c) for $t_{out} = 10^{-2}$ (*1*, *3*, and *5*) and 10^{-3} s (*2*, *4*, and *6*). The analytical calculation was made by formulas (11) (*1* – *3*), (20) (*4* and *5*), and (15) (*6*).

Table 1. Relationship between the characteristic times t_{int} and t_{out}.

t_{out}/s	$r_b = 0.1\,\mu m$	$r_b = 1\,\mu m$	$r_b = 10\,\mu m$
10^{-3}	$t_{out} \ll t_{int}$	$t_{out} \sim t_{int}$	$t_{out} \gg t_{int}$
10^{-2}	$t_{out} \sim t_{int}$	$t_{out} \gg t_{int}$	$t_{out} \gg t_{int}$

The relationships between the characteristic times t_{int} and t_{out} are conveniently collected in Table 1 for all versions of the calculations. When comparing the analytical dependences and the numerical calculations given in Fig. 1, it is pertinent to note that they diverge to some extent by the end of the laser pulse for bubbles with $r_b \leqslant 1$ μm. This is caused by the involvement of bubbles in the convective motion of the melt which is enhanced with decreasing the bubble radius.

The melt velocity is relatively low in the centre of the pool and is high at the periphery that harbours the centre of the vortex of convective melt motion. As a result, the motion of a bubble is nearly rectilinear near the pool centre and is determined by the thermocapillary force acting on the bubble. The closer to the periphery of the pool of melt, the more complex the bubble motion, because a progressively increasing frictional force acts on the bubble in addition to the thermocapillary force. A bubble that finds itself at the melt surface is carried to the periphery to reside there till its escape from the melt. However, there exists a critical region near the vortex centre which a bubble cannot, once it enters the region, escape even for $t \gg t_{int}$, with the result that a fraction of the bubbles find themselves as if 'locked' in the melt.

Fig. 2a gives the instantaneous distribution of the bubbles of radius $r_b = 1$ μm at the end of the laser pulse obtained by numerical simulation. One can easily see the bubbles that have not escaped from the melt, which reside near the centre of the thermocapillary vortex. They are precisely the primary reason why the results of analytical estimates of the egress of bubbles from the melt disagree with the numerical calculations for small-sized bubbles for long times t (Figs 1b and c).

However, these bubbles amount to only several percent of their initial number. We emphasise that this efficiency of removing microbubbles is due to the fact that they are subjected to a strong thermocapillary force in the direction of the laser beam. Given for comparison in Fig. 2b is the instantaneous distribution of the bubbles with the same dimensions as in the case of Fig. 2a, though with neglect of the thermocapillary force. The concentration of gas bubbles in the melt is substantially higher than in the previous case and amounts to $0.88\alpha_0$ at the end of the laser pulse. The velocity of thermocapillary flow at the periphery of the pool of melt is high, the frictional force between the bubbles and the melt exceeds the buoyancy force and hinder the escape of the bubbles from the pool. In the calculations, a similar situation was observed for the bubbles of size 0.01 μm and below even taking into account the thermocapillary force.

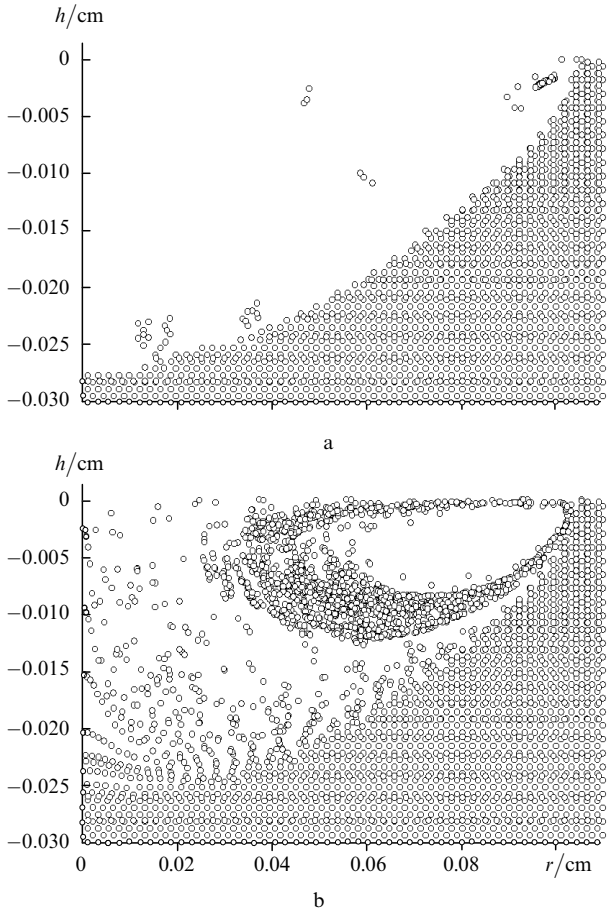

Figure 2. Distribution of gas bubbles 1 μm in radius in the sample at the moment $t = 0.1$ s with (a) and without (b) inclusion of the thermocapillary force.

4. Conclusions

Therefore, the laser degassing of surfaces is efficient for microbubbles with $r_b \geqslant 0.1$ μm. Our analysis showed that a gas bubble in the near-surface region moves, for any parameters of laser radiation, from the centre of the pool of melt to the periphery. Our analytical model yielded the principal degassing-determining condition — the relationship between the characteristic bottom-to-surface bubble drift time t_{int} and the characteristic time t_{out} of the passage of a bubble through the melt surface. For $t_{out} \geqslant t_{int}$, the egress of the gas phase from the pool of melt is determined only by the time t_{out} and is independent of the parameters of laser radiation. For $t_{out} < t_{int}$, the egress of the gas phase from the pool of melt strongly depends on the dynamics of the sample melting and, hence, on the parameters of laser radiation.

Acknowledgements. The authors are indebted to O V Khoruzhii for his constant interest in this study and useful comments. This work was supported in part by the Russian Foundation for Basic Research, Grant No. 99-02-17241.

References

1. Redchis V V, Frolov V A, Ovchinnikov V V, et al. *Fiz. Khim. Obrab. Mater.* **3** 70 (1998)
2. Kosyrev F K, Kopeliovich D Kh, Kuz'menko T G, et al. *Vopr. At. Nauki Tekh.* (3) 7 (1989)
3. Levich V G *Fiziko-Khimicheskaya Gidrodinamika (Physicochemical Hydrodynamics)* (Moscow: Fizmatgiz, 1959)
4. Sukhodol'skii A T *Izv. Akad. Nauk SSSR Ser. Fiz.* **50** 1095 (1986)
5. Povitskii A S, Lyubin L Ya *Osnovy Dinamiki i Teplomassoobmena Zhidkostei i Gazov pri Nevesomosti (Fundamentals of the Dynamics and the Heat and Mass Exchange of Liquids and Gases in Zero Gravity)* (Moscow: Mashinostroenie, 1972)
6. Young N O, Goldstein J S, Block M J *J. Fluid Mech.* **6** 350 (1959)

7. Uglov A A, Smurov I Yu, Gus'kov A G *Kvantovaya Elektron. (Moscow)* **18** 1081 (1991) [*Sov. J. Quantum Electron* **21**(9) 980 (1991)]
8. Redchis V V, Redchis A V, Frolov V A, et al. *Fiz. Khim. Obrab. Mater.* **2** 71 (1998)
9. Soo S L *Fluid Dynamics of Multiphase Systems* (Waltham, MA: Blaisdell, 1967)
10. Nigmatulin R I *Dinamika Mnogofaznykh Sred (Dynamics of Multiphase Media)* (Moscow: Nauka, 1987) vol. 1
11. Chan C L, Chen M M, Mazumder J *J. Heat Transfer* **110** 140 (1988)
12. Gladush G G, Likhanskii V V, Loboiko A I *Kvantovaya Elektron. (Moscow)* **24** 274 (1997) [*Quantum Electron* **27**(3) 268 (1997)]
13. Elkin N N, Likhanskii V V, Loboiko A I, Khorujii O V *Proc. Intern. Topical Meeting on ARS* (Pittsburgh, USA, 1994) vol. 1, p. 158